Front. Med. 2021, 15(1): 79–90
https://doi.org/10.1007/s11684-020-0783-8

RESEARCH ARTICLE

Astragaloside IV suppresses post-ischemic natural killer cell infiltration and activation in the brain: involvement of histone deacetylase inhibition

Baokai Dou[1,2], Shichun Li[1,3], Luyao Wei[1,3], Lixin Wang[1], Shiguo Zhu[1], Zhengtao Wang[2], Zunji Ke[3], Kaixian Chen (✉)[2], Zhifei Wang (✉)[1,3]

[1]*School of Basic Medical Sciences, Shanghai University of Traditional Chinese Medicine, Shanghai 201203, China;* [2]*Institute of Chinese Materia Medica, Shanghai University of Traditional Chinese Medicine, Shanghai 201203, China;* [3]*Academy of Integrative Medicine, Shanghai University of Traditional Chinese Medicine, Shanghai 201203, China*

Abstract **Natural killer (NK) cells, a type of cytotoxic lymphocytes, can infiltrate into ischemic brain and exacerbate neuronal cell death. Astragaloside IV (ASIV) is the major bioactive ingredient of *Astragalus membranaceus*, a Chinese herbal medicine, and possesses potent immunomodulatory and neuroprotective properties. This study investigated the effects of ASIV on post-ischemic brain infiltration and activation of NK cells. ASIV reduced brain infarction and alleviated functional deficits in MCAO rats, and these beneficial effects persisted for at least 7 days. Abundant NK cells infiltrated into the ischemic hemisphere on day 1 after brain ischemia, and this infiltration was suppressed by ASIV. Strikingly, ASIV reversed NK cell deficiency in the spleen and blood after brain ischemia. ASIV inhibited astrocyte-derived CCL2 upregulation and reduced $CCR2^+$ NK cell levels in the ischemic brain. Meanwhile, ASIV attenuated NK cell activating receptor NKG2D levels and reduced interferon-γ production. ASIV restored acetylation of histone H3 and the p65 subunit of nuclear factor-κB in the ischemic brain, suggesting inhibition of histone deacetylase (HDAC). Simultaneously, ASIV prevented p65 nuclear translocation. The effects of ASIV on reducing CCL2 production, restoring acetylated p65 levels and preventing p65 nuclear translocation were mimicked by valproate, an HDAC inhibitor, in astrocytes subjected to oxygen-glucose deprivation. Our findings suggest that ASIV inhibits post-ischemic NK cell brain infiltration and activation and reverses NK cell deficiency in the periphery, which together contribute to the beneficial effects of ASIV against brain ischemia. Furthermore, ASIV's effects on suppressing NK cell brain infiltration and activation may involve HDAC inhibition.**

Keywords astragaloside IV; brain ischemia; natural killer cells; histone deacetylase; nuclear factor-κB

Introduction

Stroke is the leading cause of adult long-term disability and death worldwide. About 80% strokes are ischemic. Currently, therapeutic options for ischemic stroke treatment are very limited. It is still urgent to advance the field of stroke therapy. Brain ischemia triggers inflammation and immune responses that participate in all stages of the ischemic cascade and may shape the outcome of stroke [1]. Several immunomodulatory drugs targeting key inflammatory mediators and molecules controlling lymphocyte migration and activation have been assessed in clinical trials [2]. Hence, immune intervention is a promising therapeutic strategy for stroke treatment [3].

Natural killer (NK) cells are a type of cytotoxic lymphocytes and possess the ability of coordinating innate and adaptive immune responses [4]. Abundant NK cells invade brain parenchyma within hours after stroke onset and accumulate in close proximity to ischemic neurons in stroke patients [5,6]. Ischemic neurons that lose NK cell tolerance incur NK cell-mediated killing [5]. In addition to cytolytic effects, NK cells are a major source of interferon (IFN)-γ, which induces necrosis in ischemic neurons [6].

Received December 18, 2019; accepted March 14, 2020
Correspondence: Zhifei Wang, zfwang@shutcm.edu.cn;
Kaixian Chen, kxchen@simm.ac.cn

Moreover, strategies that reduce NK cell brain infiltration abolish IFN-γ upregulation, and diminish brain infarction after brain ischemia [6]. Therefore, targeting NK cells is receiving growing attention as a potential immunomodulatory therapy for stroke [7].

Astragalus membranaceus (Huangqi) is a well-known herbal medicine and is widely used in classic prescriptions of traditional Chinese medicine in the treatment of a variety of diseases including stroke. For example, Huangqi is the monarch drug of Buyang Huanwu Decoction which is a classic herbal prescription for stroke treatment in China [8]. Clinical studies have also demonstrated the efficacy and safety of Huangqi injection (a traditional Chinese patent medicine) in the treatment of cerebral infarction [9]. Astragaloside IV (ASIV, CAS: 84687-43-4, Fig. 1A), a cycloartane triterpene saponin, is the major bioactive ingredient of Huangqi [10]. Pharmacological studies indicate that ASIV has multiple protective effects against brain ischemia, including anti-inflammation, anti-apoptosis and anti-oxidative stress [11]. In addition, ASIV possesses immunomodulatory abilities. ASIV can increase proliferation of T and B cells and antibody production, and regulate differentiation and apoptosis of activated $CD4^+$ T cells [12,13]. We have previously demonstrated that Buyang Huanwu Decoction attenuates post-ischemic brain infiltration of NK cells in a rat model of transient middle cerebral artery occlusion (MCAO) [14]. Therefore, it is likely that ASIV can suppress brain invasion and activation of NK cells following cerebral ischemia. Hence, this present study expanded on our earlier line of research and investigated whether ASIV inhibits post-ischemic NK cell infiltration and activation and protects from ischemic brain injury.

Materials and methods

MCAO surgery and drug administration

All animal experiments were performed according to the National Institutes of Health guide for the care and use of laboratory animals (NIH Publications No. 8023, revised 1978) and the protocols were approved by the Laboratory Animal Ethical Committee, Shanghai University of Traditional Chinese Medicine. Male Sprague-Dawley rats weighing 200 to 220 g (Beijing Vital River Laboratory Animal Technology Co., Ltd.) were subjected to one-hour right MCAO under inhalational anesthesia (2.5% isoflurane) followed by reperfusion as previously described [14–17]. The regional cerebral blood flow (1.5 mm posterior, 5 mm lateral to the bregma) was monitored with a laser Doppler flowmetry (Powerlab ML191, ADInstruments). MCAO rats whose regional cerebral blood flow was reduced to 27% ± 0.5% of baseline were randomized to 4 groups based on body weight: MCAO group (n = 56), MCAO + 5 mg/kg ASIV (n = 8), MCAO + 10 mg/kg ASIV (n = 8) and MCAO + 20 mg/kg ASIV (n = 56). Sham-operated rats received surgery without occlusion (n = 56). ASIV (purity > 98%, Shanghai Tauto Biotech Co., Ltd.) was intraperitoneally injected at the onset of reperfusion, 12 h later, and twice daily for up to 7 days.

Behavioral tests

The accelerating rotarod test, neurological deficit score, and gait analysis were conducted by an investigator who was blind to the treatment information on days 1, 3 and 7. For rotarod test and neurological deficit score, detailed procedures were previously described [14]. Gait analysis was performed using CatWalk 10.5 Analysis System (Noldus Information Technology, Netherlands). The constantly changing paw images were recorded by a camera placed below the glass plate across which rats walked. Each rat was required to walk across the plate at least three times without pausing. The system identified and marked each footprint, and automatically produced a series of gait statistics. Rats that were unable to complete runs due to serious deficits were excluded.

Brain infarction measurement

Brain infarction was measured and analyzed by TTC staining and ImageJ, respectively. Detailed procedures were previously described [14].

Flow cytometry

Flow cytometry was used to examine the effects of ASIV on NK cell levels in the ischemic brain, spleen and peripheral blood, and the surface expression of CCR2 and NKG2D on brain-infiltrated NK cells. Detailed procedures and gating strategies were previously described [14]. Antibodies were as follows: APC-conjugated anti-rat CD161 (BioLegend, Cat#205606), FITC-conjugated anti-rat CD3 (BioLegend, Cat#201403), PE-conjugated anti-rat CCR2 (R&D Systems, Cat#FAB8368P-100), PE-conjugated anti-rat CD314 (NKG2D, eBioscience, Cat#12-3140), and their corresponding isotype controls. FACS was performed on a BD AccuriTM C6 flow cytometer (BD Biosciences) and FlowJo (version 10) was used to analyze the data.

Primary cultures of rat cortical astrocytes and oxygen-glucose deprivation (OGD)

Cortices from 24-h newborn Sprague-Dawley rat pups were mechanically dissociated and seeded in Dulbecco's modified Eagle's medium/F12 (DMEM/F12, Gibco) supplemented with 10% fetal bovine serum (FBS, Gibco) in culture flasks pre-coated with poly-L-lysine. When cells

reached confluence, flasks were shaken at 200 rpm for 2 h at 37 °C to remove microglia and oligodendrocytes. Remaining astrocytes were trypsinized, and seeded in culture plates or dishes at 2×10^5 cells/mL. After 24 h, astrocytes were subjected to OGD. Cultures were switched to glucose-free DMEM (Gibco) and placed in an anaerobic chamber (DG250, Whitley Workstation) filled with a gas mixture of 10% H_2, 10% CO_2, and 80% N_2 at 37 °C for 4 h. After OGD, 1 g/L glucose and 10% FBS were supplemented and cells were returned to normoxic conditions for 24 h. ASIV and valproate (VPA, a histone deacetylase inhibitor) were added to the cultures 2 h before OGD at concentrations of 50 μmol/L and 5 mmol/L, respectively. Control cells were maintained in DMEM containing 1 g/L glucose for 4 h and supplemented with 10% FBS for 24 h under normoxic condition.

Immunohistochemistry and immunofluorescence staining

The infiltration of $CD161^+$ cells into the ipsilateral cortex was detected by immunohistochemistry. The expression of CCL2 and NF-κB p65 in both ischemic cortex and primary cultures of cortical astrocytes was examined by immunofluorescence staining. Detailed procedures were previously described [15,18]. The primary antibodies were as follows: mouse anti-CD161 (1:1000, Bio-Rad, Cat#MCA1427), mouse anti-CCL2 (1:1000, R&D systems, Cat#AF-479-NA), rabbit anti-GFAP (1:400, Abcam, Cat#ab7260), mouse anti-p65 (1:500, Cell Signaling Technology, Cat#6959). For immunohistochemistry, brain slices were incubated with biotinylated anti-mouse IgG (Yeasen) and then strept avidin-biotin peroxidase complex (Yeasen). The staining was visualized with a diaminobenzidine kit (Yeasen) and captured using a Zeiss AXIO Imager M2 microscope. For immunofluorescence staining, brain slices were incubated with Alexa Fluor 488 and 594-conjugated secondary antibodies (1:400, Jackson ImmunoResearch, Cat#34306ES60 and 34212ES60). Nuclei were stained with DAPI, and immunolabeling signals were captured by a Leica SP8 Confocal Microscope. ImageJ was used to quantify the results.

Real-time PCR

As previously described, total RNA from ipsilateral cortex and primary cortical astrocytes was isolated and reverse-transcribed into cDNA, and real-time PCR using SYBR green was performed [14]. Sequences of the primers were as follows: CCL2: 5′-GGACCAGAACCAAGTGAGA-3′ (sense), 5′-TGTGGAAAAGAGAGTGGATG-3′ (anti-sense); IFN-γ: 5′-GAGCATCGTAGTTGTTGGAAAT-3′ (sense) and 5′-CAGGTCTACTTTGGAGTCATTG-3′ (anti-sense). The mRNA levels were normalized against β-actin and presented as $2^{-\Delta\Delta CT}$.

ELISA

The levels of IFN-γ in the ipsilateral cortex were detected using a rat IFN-γ ELISA kit (Dakewe), as previously described [14].

Western blotting and immunoprecipitation

The protein levels of p65, histone H3, and acetyl-histone H3 (ac-H3) were detected by Western blotting as previously described [14]. Primary antibodies were as follows: mouse anti-p65 (1:1000, Cell Signaling Technology, Cat#6959), rabbit anti-histone H3 (1:1000, Abcam,), rabbit anti-ac-H3 (1:3000, Millipore, Cat#06-599) and mouse anti-β-actin (1:5000, Sigma-Aldrich, Cat#A1978). For p65, nuclear extracts were prepared using a Nuclear and Cytoplasmic Protein Extraction Kit (Beyotime). For immunoprecipitation, the lysates of the ipsilateral cortex or primary cortical astrocytes were immunoprecipitated overnight at 4 °C with mouse anti-p65 (1:50, Cell Signaling Technology, Cat#6959)/normal IgG (1:50, Santa Cruz Biotechonlogy, Cat#sc-7269), and then conjugated to nProtein A and Protein G SepharoseTM 4 Fast Flow (GE Healthcare) for 2 h at 4 °C. The complexes were washed 3 times with lysis buffer, denatured, and subjected to Western blotting to detect levels of acetyl-lysine with rabbit anti-acetyl-lysine (1:1000, Cell Signaling Technology, Cat#9441).

Statistical analysis

Statistical analysis was performed using GraphPad Prism 5. Two-way ANOVA followed by Bonferroni post-test was used to analyze the behavioral data. Comparisons between two groups and multiple groups were analyzed by Student's *t*-test and one-way ANOVA followed by Tukey's post-hoc comparisons, respectively. Data are expressed as mean ± SEM. Differences were considered statistically significant at $P < 0.05$.

Results

ASIV ameliorated functional deficits and reduced brain infarction in MCAO rats

Brain ischemia dramatically reduced the time that rats were able to stay on the accelerating rotarod on day 1 after MCAO, and this reduction lasted for at least 7 days (31 ± 13 s on day 1, 54 ± 18 s on day 3, and 40 ± 12 s on day 7, Fig. 1B). ASIV at 20 mg/kg robustly prolonged the rotarod retention time starting from day 1 in MCAO rats and this effect persisted for at least 7 days (86 ± 13 s on day 1, 117 ± 11 s on day 3, and 93 ± 11 s on day 7). ASIV at 5 or 10 mg/kg had a tendency to ameliorate this MCAO-induced motor function deficit. ASIV at all three

dosages significantly reduced the neurological deficit score of MCAO rats on day 1 after MCAO (5.3 ± 0.5 for 5 mg/kg ASIV-treated MCAO rats, 4.7 ± 0.5 for 10 mg/kg ASIV-treated MCAO rats, and 2.7 ± 0.4 for 20 mg/kg ASIV-treated MCAO rats vs. 7.1 ± 0.3 for MCAO rats; Fig. 1C). Only at 20 mg/kg did ASIV consistently ameliorate the neurological deficit score on days 3 (5.1 ± 0.5 vs. 2.5 ± 0.3) and 7 (3.4 ± 0.4 vs. 1.7 ± 0.2).

MCAO significantly impaired most gait parameters (Table 1). Among them, ASIV at 20 mg/kg markedly ameliorated MCAO-induced deficits in maximal contact area, maximal contact maximal intensity, maximal contact mean intensity, print width, print area, mean intensity, swing speed, and stride length in the left front paw of MCAO rats on day 1. Concurrently, at this dosage, ASIV also increased average speed and shortened run duration of MCAO rats. The beneficial effects of 20 mg/kg ASIV on max contact area, maximal contact maximal intensity, maximal contact mean intensity, and mean intensity persisted for at least 7 days after MCAO. ASIV at 10 mg/kg significantly increased max contact area, mean intensity, and swing speed in the left front paw of MCAO rats on day 1. However, ASIV at 5 mg/kg did not provide any protection in MCAO-induced gait deficits.

As detected by TTC staining, ASIV reduced the brain infarct volume in a dose-dependent manner on day 7 after MCAO (Fig. 1D). However, this effect was statistically significant (233.2 ± 23.9 mm^3 vs. 121.7 ± 26.2 mm^3) only at the 20 mg/kg dose. Together, ASIV at the highest dosage provided the best protective effects in MCAO-induced functional deficits and brain infarction. Therefore, 20 mg/kg was used in the subsequent animal experiments.

ASIV prevented brain-infiltration of NK cells, and reversed NK cell deficiency in the spleen and blood after brain ischemia

CD161, also known as NKR-P1, is a receptor highly expressed on NK cells [19]. On day 1 after MCAO, we observed abundant $CD161^+$ cells accumulating in the ischemic cortex, and this accumulation was diminished by ASIV treatment (Fig. 2A). These findings were further confirmed by flow cytometry in which rat NK cells were identified as $CD161^+CD3^-$ lymphocytes [14,20]. Gating strategy was as previously described [14]. NK cells comprised approximately 15% of all the infiltrated lymphocytes in the ischemic hemisphere of MCAO rats, and ASIV treatment robustly reduced the NK cell levels to 4%. Concurrent with increased lymphocyte infiltration into the ischemic area, MCAO significantly decreased NK cell levels in the spleen and blood compared with sham controls. Notably, this MCAO-induced reduction of NK cell levels in the periphery was suppressed by ASIV (Fig. 2B).

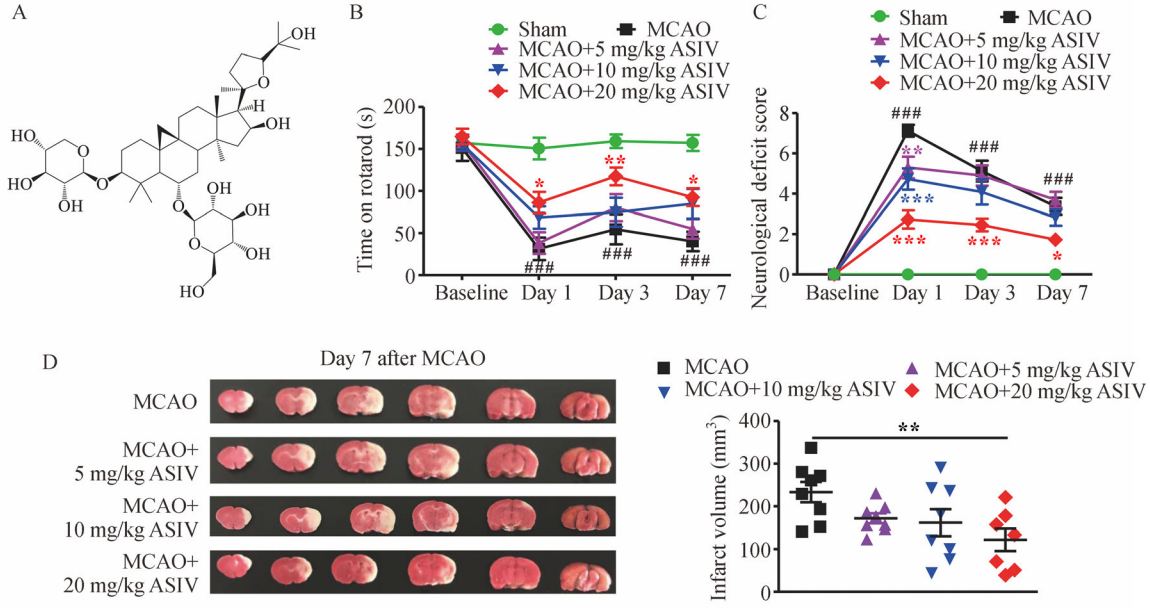

Fig. 1 ASIV improved functional deficits and reduced cerebral infarction in MCAO rats. (A) The chemical structure of ASIV. (B) ASIV at 20 mg/kg robustly increased the rotarod retention time of MCAO rats, and this effect persisted for at least 7 days after MCAO. (C) ASIV at 5, 10, and 20 mg/kg markedly reduced neurological deficit score of MCAO rats on day 1, and ASIV at the highest dosage consistently provided protection for at least 7 days. (D) ASIV dose-dependently reduced brain infarct volume in MCAO rats on day 7. $^{\#}P < 0.05$, $^{\#\#}P < 0.01$, $^{\#\#\#}P < 0.001$ vs. sham; $^{*}P < 0.05$, $^{**}P < 0.01$, $^{***}P < 0.001$ vs. MCAO; $n = 8$.

Table 1 ASIV ameliorated gait deficits in MCAO rats

Parameter	Day	Sham	MCAO	MCAO + 5 mg/kg ASIV	MCAO + 10 mg/kg ASIV	MCAO + 20 mg/kg ASIV
Max contact area (mm^2)	1	118.2±12.0	56.6±9.3$^{\#\#\#}$	77.3±12.4	97.8±10.2*	97.8±6.7**
	3	110.1±8.4	78.4±5.8$^{\#}$	95.7±10.1	102.1±6.5	105.3±7.6*
	7	123.5±5.3	71.8±10.6$^{\#\#\#}$	92.2±10.8	80.9±9.7	107.5±6.6**
Max contact max intensity	1	188.1±6.1	134.5±12.6$^{\#\#}$	155.9±11.4	175.7±9.5	176.9±9.1*
	3	199.9±4.1	165.5±10.9$^{\#}$	181.7±18.8	190.3±2.7	193.0±5.8*
	7	203.0±2.2	166.6±16.2$^{\#\#}$	184.4±7.7	176.1±12.7	197.9±2.3*
Max contact mean intensity	1	85.1±3.2	64.4±3.1$^{\#\#}$	72.9±3.0	79.7±4.2	78.1±3.7*
	3	86.2±2.3	74.4±2.4$^{\#}$	81.0±4.5	82.9±1.6	84.9±2.6*
	7	88.7±2.6	73.9±4.2$^{\#\#}$	78.9±3.2	76.3±3.8	84.9±1.9*
Print width (mm)	1	20.2±0.7	12.2±0.9$^{\#\#\#}$	13.2±1.6	15.0±0.6	16.4±0.6**
	3	19.1±0.6	16.1±0.7	17.8±1.5	17.2±0.7	18.4±0.4
	7	21.6±1.0	17.9±0.8	20.1±0.6	19.1±0.3	19.7±0.6
Print area (mm^2)	1	133.2±5.1	75.8±11.1$^{\#}$	90.5±13.8	115.5±9.9	125.0±12.4*
	3	131.6±9.6	91.5±6.1	109.3±10.6	118.2±8.0	119.7±8.2
	7	151.2±15.0	96.7±11.2	111.7±11.6	94.3±11.0	128.1±8.8
Mean intensity	1	87.9±2.6	67.4±2.7$^{\#\#}$	74.8±3.5	83±4.4*	81.4±3.8*
	3	90.6±2.3	79.7±2.1$^{\#}$	85.0±5.3	87.5±1.7	89.6±2.8*
	7	92.9±2.3	77.6±4.6$^{\#\#}$	83.1±3.2	80.1±4.1	89.4±1.9*
Swing speed (mm/s)	1	964.5±75.4	568.1±86.1$^{\#\#}$	846.6±147.1	845.6±22.0*	893.2±54.5**
	3	1011.2±73.1	809.8±82.2	1036.1±62.7	952.7±60.5	929.0±50.7
	7	1024.5±111.8	897.7±46.1	1097.1±60.1	852.4±60.8	958.9±37.4
Stride length (mm)	1	123.0±5.5	86.0±3.5$^{\#\#\#}$	93.9±5.6	102.0±7.8	110.6±5.4**
	3	128.8±7.1	117.0±7.9	132.1±6.1	132.1±6.4	123.0±4.9
	7	119.8±5.4	128.9±5.1	132.4±5.9	114.9±8.2	133.9±5.8
Duration (s)	1	1.2±0.1	2.5±0.2$^{\#\#\#}$	2.2±0.2	1.8±0.2	1.6±0.1**
	3	1.2±0.2	1.8±0.2	1.1±0.1	1.3±0.1	1.5±0.2
	7	1.4±0.2	1.3±0.1	1.2±0.1	1.4±0.1	1.2±0.1
Average speed (mm/s)	1	343.6±24.4	158.1±16.9$^{\#\#\#}$	178.5±16.5	232.9±21.3	258.4±25.5*
	3	319.1±29.7	253.7±32.1	360.9±18.8	318.8±30.4	292.3±21.7
	7	298.4±28.4	310.5±24.3	352.4±24.4	297.1±16.5	334.3±20.0

$^{\#}P<0.05$, $^{\#\#}P<0.01$, $^{\#\#\#}P<0.001$ vs. sham; $^{*}P<0.05$, $^{**}P<0.01$ vs. MCAO; $n = 8$.

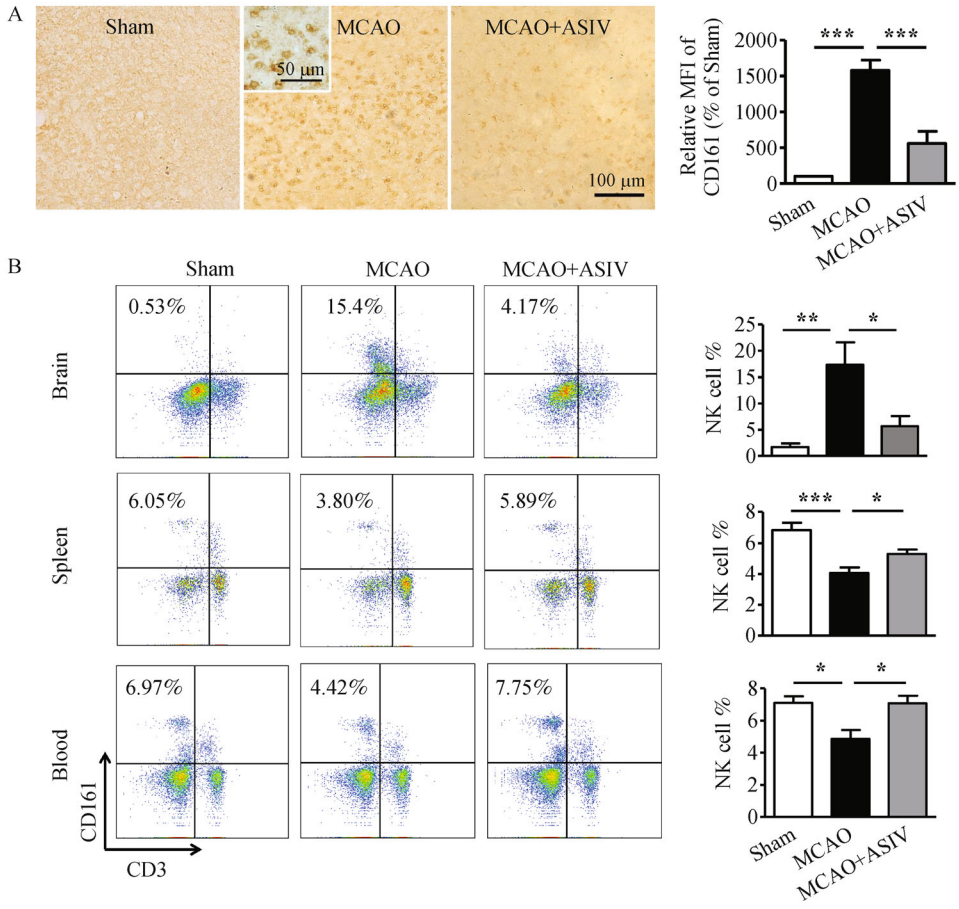

Fig. 2 ASIV suppressed brain infiltration of NK cells and reversed NK cell deficiency in the periphery after brain ischemia. (A) As assessed by immunohistochemistry, abundant $CD161^+$ cells were accumulated in the ischemic cortex and this accumulation was robustly inhibited by ASIV. (B) Flow cytometry revealed that ASIV markedly suppressed the infiltration of NK cells ($CD161^+CD3^-$) into the ischemic hemisphere. Simultaneously, the NK cell levels were significantly decreased in the spleen and blood after brain ischemia, which were restored by ASIV treatment. $^{***}P < 0.001$, $^{**}P < 0.01$, $^{*}P < 0.05$, $n = 8$.

ASIV downregulated CCL2 in the ischemic brain and CCR2 on brain-infiltrated NK cells

CCL2 is one of the major chemokines recruiting immune cells into the ischemic brain. As expected, CCL2 mRNA expression increased 175-fold in the ischemic cortex on day 1 after MCAO compared with sham controls, and ASIV robustly reduced this to 60-fold (Fig. 3A). As revealed by immunofluorescence staining, CCL2 was barely detected in the cortex of sham-operated rats. In contrast, abundant CCL2 protein was observed in the ischemic cortex of MCAO rats, and this upregulation was markedly suppressed by ASIV treatment (8-fold vs. 3.5-fold, Fig. 3B). CCL2 in the ischemic cortex was colocalized with astrocytes (Fig. 3C), but not with neurons, microglia or endothelial cells (data not shown).

CCR2 is the receptor for CCL2. We further studied whether ASIV affected $CCR2^+$ NK cell levels in the ischemic brain on day 1 after MCAO. CCR2 on NK cells was identified as $CD161^+CD3^-CCR2^+$ cells using flow cytometry (Fig. 3D). There was an 18-fold increase in $CCR2^+$ NK cell levels in the ischemic brain compared with sham controls, and this upregulation was robustly reduced to 4-fold by ASIV treatment.

ASIV inhibited IFN-γ production in the ischemic brain and NKG2D expression on brain-infiltrated NK cells

NK cell is a major source of IFN-γ that can augment brain infarction [5]. Both mRNA and protein levels of IFN-γ were significantly increased in the ischemic cortex on day 1 after MCAO (Fig. 4A and 4B). ASIV markedly reduced the mRNA expression of IFN-γ from 7-fold to 2-fold compared with sham-operated rats, and nearly completely inhibited the secretion of IFN-γ in the ischemic brain.

We further investigated the effects of ASIV on $NKG2D^+$ NK cells in the ischemic brain on day 1 after MCAO. NKG2D on NK cells was identified as

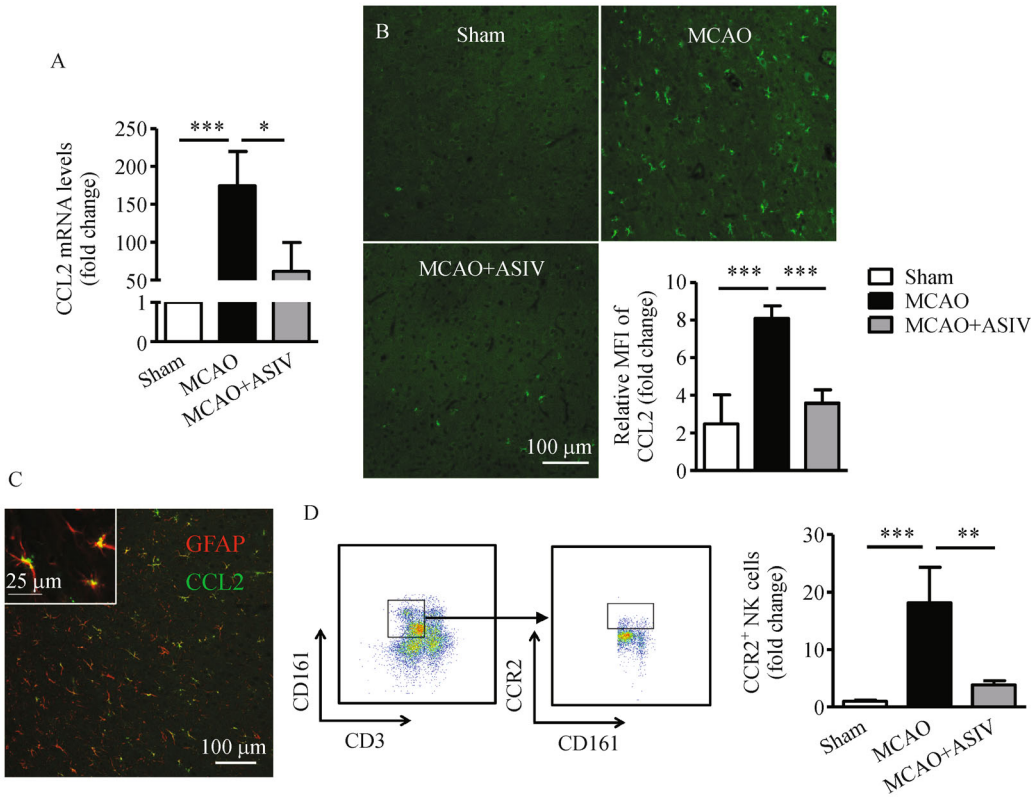

Fig. 3 ASIV downregulated CCL2 and CCR2 in the ischemic brain and on brain-infiltrated NK cells, respectively. (A) ASIV significantly reduced MCAO-induced upregulation of CCL2 mRNA levels. (B) Abundant CCL2 was observed in the ischemic cortex and this upregulation was markedly suppressed by ASIV. (C) CCL2 was colocalized with astrocytes in the ischemic bran. (D) ASIV markedly suppressed $CCR2^+$ NK cell levels in the ischemic brain. $^{***}P < 0.001$, $^{**}P < 0.01$, $^{*}P < 0.05$, $n = 8$.

$CD161^+CD3^-NKG2D^+$ cells using flow cytometry (Fig. 4C). MCAO induced a significant increase in $NKG2D^+$ NK cell levels in the ischemic brain, and this increase was markedly suppressed by ASIV treatment (7.5-fold vs. 4-fold compared with sham controls, Fig. 4C).

ASIV increased acetylation of histone H3 and NF-κB p65, and inhibited p65 nuclear translocation in the ischemic brain

Ac-H3 levels were markedly reduced in the ischemic cortex on day 1 after MCAO and were restored by ASIV treatment (Fig. 5A). To evaluate the effects of ASIV on acetylation of p65 (ac-p65) in the ischemic brain, p65 was immunoprecipitated and then subjected to Western blotting using anti-acetyl-lysine antibody. On day 1 after MCAO, ac-p65 levels in the ischemic cortex were reduced to half of those in sham controls, and were significantly restored by ASIV (Fig. 5B). Concurrently, as detected by Western blotting, MCAO-induced nuclear translocation of p65 was markedly inhibited by ASIV treatment (Fig. 5C). The inhibitory effects of ASIV on MCAO-induced p65 nuclear translocation were confirmed by staining p65 with DAPI in the ischemic cortex (Fig. 5D).

ASIV and VPA reduced CCL2 expression, restored ac-p65 levels, and inhibited p65 nuclear translocation in primary cultures of rat cortical astrocytes after OGD insult

As aforementioned, CCL2 was mainly produced by astrocytes in the ischemic cortex (Fig. 3C). We investigated the effects of ASIV and VPA, a histone deacetylase (HDAC) inhibitor, on CCL2 production, ac-p65 levels and p65 nuclear translocation in OGD-treated primary cortical astrocytes. Compared with control cells, the mRNA levels of CCL2 increased more than 4-fold in astrocytes after OGD insult, and this upregulation was reduced to 2-fold by 50 μmol/L ASIV and to a level similar to that in control cells by 5 mmol/L VPA (Fig. 6A). Consistent with the effects on mRNA levels, ASIV and VPA robustly suppressed OGD-upregulated CCL2 protein expression (17-fold compared with control cells) in astrocyte cultures (9.5-fold for ASIV and 4-fold for VPA, Fig. 6B and 6C).

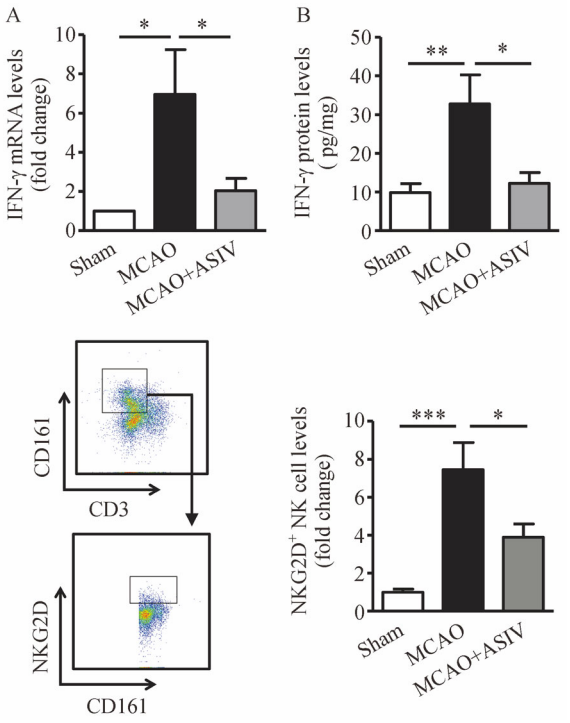

Fig. 4 ASIV decreased IFN-γ production in the ischemia cortex and NKG2D expression on brain-infiltrated NK cells. (A, B) Both mRNA and protein levels of IFN-γ were markedly increased in the ischemic cortex and were robustly reduced by ASIV. (C) NKG2D$^+$ NK cell levels were increased in the ischemic brain and were significantly reduced by ASIV. ***$P < 0.001$, **$P < 0.01$, *$P < 0.05$, $n = 8$.

As expected, OGD induced a marked decrease of ac-p65 levels in astrocytes, and this reduction was significantly inhibited by ASIV and completely reversed by VPA (Fig. 6D). Furthermore, ASIV and VPA robustly inhibited the nuclear translocation of p65 in OGD-treated astrocytes, as revealed by immunofluorescence staining (Fig. 6E).

Discussion

This study demonstrated that ASIV suppressed the brain infiltration and activation of NK cells and reversed NK cell deficiency in the periphery in MCAO rats, which together contribute to the beneficial effects of ASIV against brain ischemia. ASIV's inhibitory effects on NK cell brain infiltration and activation may involve HDAC inhibition.

Ischemic brain cells can recruit NK cells that breach blood-brain barrier integrity, accelerate neuronal cell death, and worsen ischemic outcomes [5,6]. The present study showed that ASIV markedly suppressed NK cell infiltration and activation in the ischemic brain and these effects echoed those of Buyang Huanwu Decoction [14]. ASIV is the representative bioactive component of Huangqi which is the monarch drug of Buyang Huanwu Decoction. Hence, our findings suggest that ASIV may be the key component of Buyang Huanwu Decoction that possesses the ability of suppressing post-ischemic NK cell brain infiltration and activation.

CCL2 is one of the major chemokines expressed in brain cells in response to cerebral ischemia. Chemotaxis mediated by CCL2 and its receptor CCR2 plays a pivotal role in post-ischemic brain recruitment of immune cells [21]. CCL2 upregulation starts within hours, and lasts for days after brain ischemia [22]. CCL2-deficient mice have reduced neuroinflammation, immune cell infiltration, blood-brain barrier breakdown, and brain infarction, and similar phenomena are also observed in CCR2-deficient mice [23–25]. In agreement with these findings, we found that CCL2 mRNA and protein levels were dramatically increased in the ischemic brain on Day 1 after MCAO. Both *in vivo* and *in vitro* results suggested that CCL2 was mainly expressed in astrocytes in the current experimental paradigm. Simultaneously, brain ischemia robustly increased CCR2$^+$ NK cell levels in the ischemic brain in response to upregulated CCL2. Notably, ASIV not only markedly suppressed CCL2 upregulation but also reduced CCR2$^+$ NK cell levels in the ischemic brain. Our findings suggested that ASIV may attenuate brain infiltration of NK cells via suppression of CCL2/CCR2-mediated chemotaxis after brain ischemia.

NF-κB is a key transcription factor regulating expression of a variety of cytokines and chemokines including CCL2 [26]. Accumulating evidence suggests that post-translational acetylation of NF-κB, especially at the p65 subunit, plays an important role in regulating NF-κB activation [27]. Seven lysine residues have been identified to be reversibly acetylated within p65, including K122, K123, K218, K221, K310, K314, and K315. Notably, acetylation at K122, K123, K314, and K315 negatively regulates NF-κB-mediated transcription, whereas acetylation at the other sites enhances its activation [27]. In the present study, concurrent with the activation of NF-κB, the total acetylation levels of p65 were dramatically decreased in the ischemic cortex and OGD-treated astrocytes. These results suggest that brain ischemia may inhibit acetylation of p65 at K122, K123, K314, and K315.

HDACs can deacetylate lysine residues of histones and non-histone proteins, and control a wide variety of cellular functions beyond epigenetic mechanism. Lysine residues of p65 can be deacetylated by HDACs [27–30]. Increased acetylation of histones is an index of HDAC inhibition [31]. We found that ASIV prevented the reduction of ac-H3 levels in the ischemic cortex. Furthermore, ASIV restored ac-p65 levels, inhibited p65 nuclear translocation and downregulated CCL2 in both ischemic brain and OGD-treated astrocytes, and these effects of ASIV were mimicked by VPA, an HDAC inhibitor. Together, these findings suggest that the mechanism underlying the effects of ASIV on suppression of post-ischemic brain-recruitment of NK cells may involve HDAC-inhibition-mediated

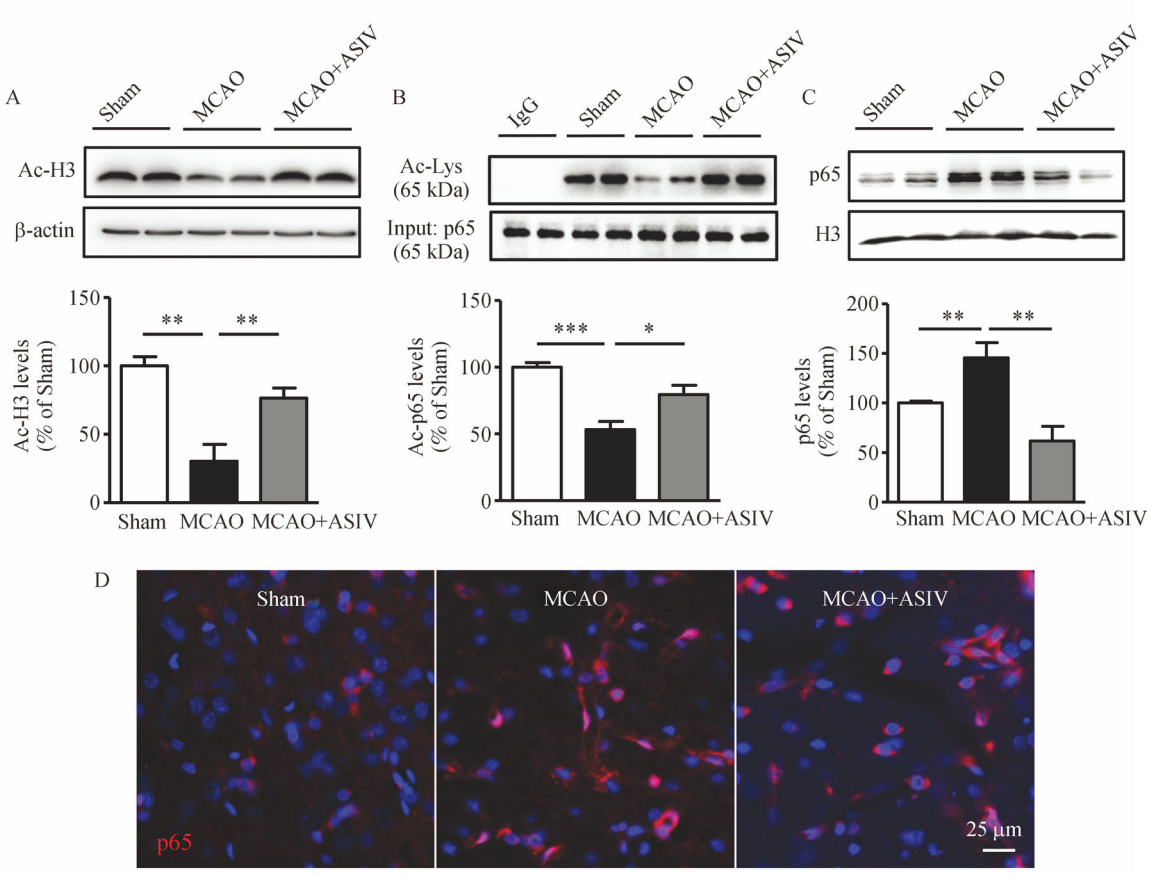

Fig. 5 ASIV increased acetylation of histone H3 and p65, and inhibited p65 nuclear translocation in the ischemic brain. (A) ASIV restored ac-H3 levels in the ischemic cortex. (B) ASIV significantly increased ac-p65 levels in the ischemic cortex. (C, D) MCAO-induced nuclear translocation of p65 was markedly inhibited by ASIV, as assessed by Western blotting and immunofluorescent staining, respectively. ***$P < 0.001$, **$P < 0.01$, *$P < 0.05$, $n = 8$.

blockade of NF-κB activation and the subsequent down-regulation of CCL2.

Activated NK cells can boost local inflammation through secretion of proinflammatory cytokines, such as IFN-γ. Previous studies have suggested that NK cell-derived IFN-γ may induce necrosis in neurons and exacerbate stroke outcomes in transient MCAO mice [5,32]. The present study showed that both mRNA and protein levels of IFN-γ were significantly upregulated in the ischemic cortex in rats, and ASIV nearly completely inhibited MCAO-induced IFN-γ upregulation. NKG2D, an important activating receptor on NK cells, can stimulate cytokine secretion and activate NK cell cytolytic responses [33]. The loss of NK cell tolerance in ischemic neurons is partially attributed to upregulation of NKG2D on NK cells in the ischemic brain [5]. Consistent with this notion, we found a significant increase of $NKG2D^+$ NK cells in the ischemic hemisphere, and this increase was markedly reduced by ASIV treatment. Hence, our findings suggest that ASIV may suppress activation of brain-infiltrated NK cells through downregulating IFN-γ production and NKG2D expression following brain ischemia.

HDACs are key factors regulating the function of immune cells [34]. In addition to modulating NK cell infiltration through p65 deacetylation, HDACs may also be involved in the effects of ASIV on regulating NK cell activation. HDAC inhibition can upregulate NKG2D in NK and γδT cells to enhance their recognition of cancer cells [35,36]. Moreover, VPA has been shown to inhibit NKG2D expression in NK cells [37]. The discrepancy of regulating NKG2D expression may be attributed to involvement of different HDAC isoforms. However, the HDAC isoform involved in the effects of ASIV on post-ischemic NK cell infiltration and activation remains unclear. Notably, HDAC3 inhibition has been shown to downregulate NKG2D expression on NK cells through suppression of STAT3 [37]. Furthermore, the involvement of HDAC3 has been suggested in the deacetylation of p65 at K122, K123, K314, and K315, and subsequent NF-κB activation [38,39]. Inhibition of HDAC3 by VPA has been

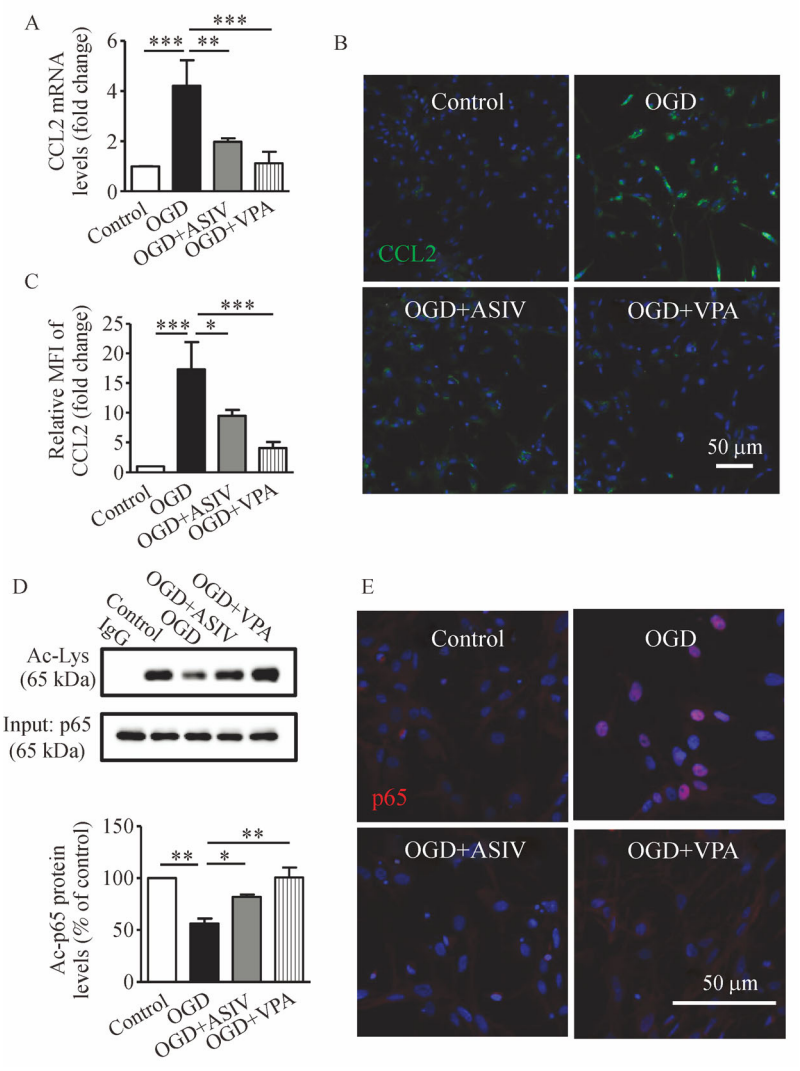

Fig. 6 ASIV and VPA reduced CCL2 expression, restored p65 acetylation, and inhibited p65 nuclear translocation in OGD-treated primary cultures of rat cortical astrocyte. (A–C) OGD-induced upregulation in CCL2 mRNA levels and protein expression in astrocytes was reduced by ASIV and VPA. (D) ASIV and VPA restored the acetylation of p65 in OGD-treated astrocytes. (E) ASIV and VPA inhibited the nuclear translocation of p65 in OGD-treated astrocytes. ***$P < 0.001$, **$P < 0.01$, *$P < 0.05$, $n = 3$.

shown to upregulate p65 acetylation, inhibit NF-κB activation, and attenuate inflammatory responses [36]. Therefore, the post-ischemic protection of ASIV which we observed may be due to inhibition of HDAC3 and suppression of brain infiltration and activation of NK cells. This notion requires further investigation.

Brain ischemia triggers peripheral immunosuppression that leads to post-stroke infections, such as pneumonia, a major cause of death in stroke patients [40]. Stroke-induced peripheral immunosuppression is mainly caused by lymphocyte apoptosis mediated through the sympathetic nervous system and hypothalamic-pituitary-adrenal axis [41]. Studies from our laboratory and others have demonstrated that peripheral NK cell numbers are decreased in stroke patients and MCAO rodents [14,41]. In line with these findings, the present study observed a significant reduction in NK cell levels in both spleen and blood of MCAO rats. Strikingly, ASIV restored the peripheral NK cell levels in MCAO rats. ASIV has been shown to promote proliferation of T cells and B cells in mouse spleen, and suppress lymphocyte apoptosis in thymus and spleen in septic mice [12,42]. These findings suggest that ASIV may inhibit apoptosis and stimulate proliferation of NK cells in the periphery, which suppress the peripheral NK cell deficiency observed after ischemic stroke. The mechanism underlying the distinct effects ASIV on NK cell levels in the brain and periphery after brain ischemia is under investigation in our laboratory.

In conclusion, ASIV inhibited the infiltration and activation of NK cells in the ischemic brain, and the

underlying mechanism may involve HDAC inhibition. It is also interesting to note that ASIV reversed the MCAO-induced NK cell deficiency in the periphery, suggesting that ASIV may suppress post-ischemic peripheral immunodeficiency. The distinct effects of ASIV on NK cells in the brain and periphery may contribute to the overall beneficial effects of ASIV in ischemic rats, and indicate the clinical efficacy and safety of this drug. Our findings suggest that the NK cell is a promising target for the treatment of ischemic stroke and pave the way for potential clinical trials of ASIV.

Acknowledgements

This study was supported by the National Natural Science Foundation of China (Nos. 81503055 and 81873029) and Shanghai Youth Eastern Scholar (No. QD2015037). The authors thank Mr. Peter Leeds (National Institutes Health, USA) for his editorial assistance.

Compliance with ethics guidelines

Baokai Dou, Shichun Li, Luyao Wei, Lixin Wang, Shiguo Zhu, Zhengtao Wang, Zunji Ke, Kaixian Chen, and Zhifei Wang declare no conflict of interest. All institutional and national guidelines for the care and use of laboratory animals were followed.

References

1. Shi K, Tian DC, Li ZG, Ducruet AF, Lawton MT, Shi FD. Global brain inflammation in stroke. Lancet Neurol 2019; 18(11): 1058–1066
2. Fu Y, Liu Q, Anrather J, Shi FD. Immune interventions in stroke. Nat Rev Neurol 2015; 11(9): 524–535
3. Iadecola C, Anrather J. The immunology of stroke: from mechanisms to translation. Nat Med 2011; 17(7): 796–808
4. Vivier E, Raulet DH, Moretta A, Caligiuri MA, Zitvogel L, Lanier LL, Yokoyama WM, Ugolini S. Innate or adaptive immunity? The example of natural killer cells. Science 2011; 331(6013): 44–49
5. Gan Y, Liu Q, Wu W, Yin JX, Bai XF, Shen R, Wang Y, Chen J, La Cava A, Poursine-Laurent J, Yokoyama W, Shi FD. Ischemic neurons recruit natural killer cells that accelerate brain infarction. Proc Natl Acad Sci USA 2014; 111(7): 2704–2709
6. Zhang Y, Gao Z, Wang D, Zhang T, Sun B, Mu L, Wang J, Liu Y, Kong Q, Liu X, Zhang Y, Zhang H, He J, Li H, Wang G. Accumulation of natural killer cells in ischemic brain tissues and the chemotactic effect of IP-10. J Neuroinflammation 2014; 11(1): 79
7. Chen C, Ai QD, Chu SF, Zhang Z, Chen NH. NK cells in cerebral ischemia. Biomed Pharmacother 2019; 109: 547–554
8. Hao CZ, Wu F, Shen J, Lu L, Fu DL, Liao WJ, Zheng GQ. Clinical efficacy and safety of Buyang Huanwu Decoction for acute ischemic stroke: a systematic review and meta-analysis of 19 randomized controlled trials. Evid Based Complement Alternat Med 2012; 2012: 630124
9. Duan X, Wu J, Wang K, Liu S, Zhang D, Zhang X, Zhang B. Meta-analysis of efficacy of Huangqi Injection in the treatment of cerebral infarction. Chin J Pharmacoepidemiol (Yao Wu Liu Xing Bing Xue Za Zhi) 2017; (9): 607–612 (in Chinese)
10. Lai PK, Chan JY, Cheng L, Lau CP, Han SQ, Leung PC, Fung KP, Lau CB. Isolation of anti-inflammatory fractions and compounds from the root of *Astragalus membranaceus*. Phytother Res 2013; 27 (4): 581–587
11. Wang HL, Zhou QH, Xu MB, Zhou XL, Zheng GQ. Astragaloside IV for experimental focal cerebral ischemia: preclinical evidence and possible mechanisms. Oxid Med Cell Longev 2017; 2017: 8424326
12. Wang YP, Li XY, Song CQ, Hu ZB. Effect of astragaloside IV on T, B lymphocyte proliferation and peritoneal macrophage function in mice. Acta Pharmacol Sin 2002; 23(3): 263–266
13. Yang L, Xing F, Han X, Li Q, Wu H, Shi H, Wang Z, Huang F, Wu X. Astragaloside IV regulates differentiation and induces apoptosis of activated $CD4^+$ T cells in the pathogenesis of experimental autoimmune encephalomyelitis. Toxicol Appl Pharmacol 2019; 362: 105–115
14. Dou B, Zhou W, Li S, Wang L, Wu X, Li Y, Guan H, Wang C, Zhu S, Ke Z, Huang C, Wang Z. Buyang Huanwu Decoction attenuates infiltration of natural killer cells and protects against ischemic brain injury. Cell Physiol Biochem 2018; 50(4): 1286–1300
15. Wang Z, Leng Y, Wang J, Liao HM, Bergman J, Leeds P, Kozikowski A, Chuang DM. Tubastatin A, an HDAC6 inhibitor, alleviates stroke-induced brain infarction and functional deficits: potential roles of α-tubulin acetylation and FGF-21 up-regulation. Sci Rep 2016; 6(1): 19626
16. Wang Z, Tsai LK, Munasinghe J, Leng Y, Fessler EB, Chibane F, Leeds P, Chuang DM. Chronic valproate treatment enhances postischemic angiogenesis and promotes functional recovery in a rat model of ischemic stroke. Stroke 2012; 43(9): 2430–2436
17. Wang Z, Leng Y, Tsai LK, Leeds P, Chuang DM. Valproic acid attenuates blood-brain barrier disruption in a rat model of transient focal cerebral ischemia: the roles of HDAC and MMP-9 inhibition. J Cereb Blood Flow Metab 2011; 31(1): 52–57
18. Wang ZF, Tang XC. Huperzine A protects C6 rat glioma cells against oxygen-glucose deprivation-induced injury. FEBS Lett 2007; 581(4): 596–602
19. Giorda R, Rudert WA, Vavassori C, Chambers WH, Hiserodt JC, Trucco M. NKR-P1, a signal transduction molecule on natural killer cells. Science 1990; 249(4974): 1298–1300
20. Lehmann J, Härtig W, Seidel A, Füldner C, Hobohm C, Grosche J, Krueger M, Michalski D. Inflammatory cell recruitment after experimental thromboembolic stroke in rats. Neuroscience 2014; 279: 139–154
21. Mirabelli-Badenier M, Braunersreuther V, Viviani GL, Dallegri F, Quercioli A, Veneselli E, Mach F, Montecucco F. CC and CXC chemokines are pivotal mediators of cerebral injury in ischaemic stroke. Thromb Haemost 2011; 105(3): 409–420
22. Wang X, Yue TL, Barone FC, Feuerstein GZ. Monocyte chemoattractant protein-1 messenger RNA expression in rat ischemic cortex. Stroke 1995; 26(4): 661–666
23. Hughes PM, Allegrini PR, Rudin M, Perry VH, Mir AK, Wiessner C. Monocyte chemoattractant protein-1 deficiency is protective in a murine stroke model. J Cereb Blood Flow Metab 2002; 22(3): 308–317

24. Dimitrijevic OB, Stamatovic SM, Keep RF, Andjelkovic AV. Absence of the chemokine receptor CCR2 protects against cerebral ischemia/reperfusion injury in mice. Stroke 2007; 38(4): 1345–1353
25. Strecker JK, Minnerup J, Schütte-Nütgen K, Gess B, Schäbitz WR, Schilling M. Monocyte chemoattractant protein-1-deficiency results in altered blood-brain barrier breakdown after experimental stroke. Stroke 2013; 44(9): 2536–2544
26. Ueda A, Okuda K, Ohno S, Shirai A, Igarashi T, Matsunaga K, Fukushima J, Kawamoto S, Ishigatsubo Y, Okubo T. NF-κB and Sp1 regulate transcription of the human monocyte chemoattractant protein-1 gene. J Immunol 1994; 153(5): 2052–2063
27. Huang B, Yang XD, Lamb A, Chen LF. Posttranslational modifications of NF-κB: another layer of regulation for NF-κB signaling pathway. Cell Signal 2010; 22(9): 1282–1290
28. Yeung F, Hoberg JE, Ramsey CS, Keller MD, Jones DR, Frye RA, Mayo MW. Modulation of NF-κB-dependent transcription and cell survival by the SIRT1 deacetylase. EMBO J 2004; 23(12): 2369–2380
29. Liu Y, Smith PW, Jones DR. Breast cancer metastasis suppressor 1 functions as a corepressor by enhancing histone deacetylase 1-mediated deacetylation of RelA/p65 and promoting apoptosis. Mol Cell Biol 2006; 26(23): 8683–8696
30. Chen Lf, Fischle W, Verdin E, Greene WC. Duration of nuclear NF-κB action regulated by reversible acetylation. Science 2001; 293 (5535): 1653–1657
31. Seto E, Yoshida M. Erasers of histone acetylation: the histone deacetylase enzymes. Cold Spring Harb Perspect Biol 2014; 6(4): a018713
32. Yilmaz G, Arumugam TV, Stokes KY, Granger DN. Role of T lymphocytes and interferon-γ in ischemic stroke. Circulation 2006; 113(17): 2105–2112
33. Bauer S, Groh V, Wu J, Steinle A, Phillips JH, Lanier LL, Spies T. Activation of NK cells and T cells by NKG2D, a receptor for stress-inducible MICA. Science 1999; 285(5428): 727–729
34. Ellmeier W, Seiser C. Histone deacetylase function in $CD4^+$ T cells. Nat Rev Immunol 2018; 18(10): 617–634
35. Bhat J, Dubin S, Dananberg A, Quabius ES, Fritsch J, Dowds CM, Saxena A, Chitadze G, Lettau M, Kabelitz D. Histone deacetylase inhibitor modulates NKG2D receptor expression and memory phenotype of human γ/δ T cells upon interaction with tumor cells. Front Immunol 2019; 10: 569
36. López-Cobo S, Pieper N, Campos-Silva C, García-Cuesta EM, Reyburn HT, Paschen A, Valés-Gómez M. Impaired NK cell recognition of vemurafenib-treated melanoma cells is overcome by simultaneous application of histone deacetylase inhibitors. OncoImmunology 2017; 7(2): e1392426
37. Ni L, Wang L, Yao C, Ni Z, Liu F, Gong C, Zhu X, Yan X, Watowich SS, Lee DA, Zhu S. The histone deacetylase inhibitor valproic acid inhibits NKG2D expression in natural killer cells through suppression of STAT3 and HDAC3. Sci Rep 2017; 7: 45266
38. Ziesché E, Kettner-Buhrow D, Weber A, Wittwer T, Jurida L, Soelch J, Müller H, Newel D, Kronich P, Schneider H, Dittrich-Breiholz O, Bhaskara S, Hiebert SW, Hottiger MO, Li H, Burstein E, Schmitz ML, Kracht M. The coactivator role of histone deacetylase 3 in IL-1-signaling involves deacetylation of p65 NF-κB. Nucleic Acids Res 2013; 41(1): 90–109
39. Leus NG, Zwinderman MR, Dekker FJ. Histone deacetylase 3 (HDAC 3) as emerging drug target in NF-κB-mediated inflammation. Curr Opin Chem Biol 2016; 33: 160–168
40. Meisel C, Meisel A. Suppressing immunosuppression after stroke. N Engl J Med 2011; 365(22): 2134–2136
41. Liu Q, Jin WN, Liu Y, Shi K, Sun H, Zhang F, Zhang C, Gonzales RJ, Sheth KN, La Cava A, Shi FD. Brain ischemia suppresses immunity in the periphery and brain via different neurogenic innervations. Immunity 2017; 46(3): 474–487
42. Liu R, Jiang H, Tian Y, Zhao W, Wu X. Astragaloside IV protects against polymicrobial sepsis through inhibiting inflammatory response and apoptosis of lymphocytes. J Surg Res 2016; 200(1): 315–323